Evaluating the Importance of Concurrent Packet Communication in Wireless Networks

USC/ISI Technical Report ISI-TR-639, April 2007

Dongjin Son[1,2] Bhaskar Krishnamachari[1] John Heidemann[2]
{dongjins, bkrishna}@usc.edu, johnh@isi.edu
[1]Department of Electrical Engineering-Systems, [2]Information Sciences Institute
Viterbi School of Engineering, University of Southern California

Abstract

Nearly all wireless media-access (MAC) protocols are designed today with the very conservative assumption that concurrent transmissions should be prevented, because sender-receiver pairs within radio range sending on the same channel will corrupt each other's communication. While recent work has suggested that channel capture effects can be significant in reality, this paper presents the first systematic study to quantify the impact of these effects on the ability to have concurrent communications among two sender-receiver pairs that are within range of each other. We first derive a simple decision rule to determine when such concurrent communication is possible while minimizing transmission power. Through a comprehensive set of realistic simulations, we then systematically quantify the feasibility of concurrent communication with and without transmission power control as many radio and environmental parameters vary, including node position, mean and variance of path loss, signal-to-interference-plus-noise-ratio threshold ($SINR_\theta$) for packet reception, granularity and range of transmission power control. Our simulations show that often, 40–75% of the time depending primarily on distance and location, two pairs of nodes can communicate concurrently without loss even if both transmitters are within the radio sensing range of both receivers. We can observe large CTXable region with fixed transmit power, but dynamic power control significantly improves concurrent communications. Finally, at least one transmitter can almost always capture the channel in the event of concurrent transmissions, so the cost of failed attempts to CTX are minimal. We validate our simulations with testbed experiments using MicaZ motes, confirming that concurrent communication is possible to a very significant extent in real systems. These results suggest that CSMA with RTS/CTS is overly conservative and there are often gains to be realized by abandoning it.

This research is supported partially by the National Science Foundation (NSF) through the following grants: CNS-0435505, CNS-0347621, CCF-0430061, CNS-0325875, NeTS-NOSS-0435517 (SNUSE), CNS-0626702 (SISS), and in part by funding from Bosch Research and by a hardware donation from Intel Corporation.

Contributions	Section
CTXable link and optimal Tx power decision rule	4
New metric for *CTXability* (concurrent communication)	5.2
Quantification of CTXability: User Controllable parameters	
Higher Tx power increases *CTXability* for fixed power	5.3
Shorter link distance increases *CTXability*	5.4.1
Lower SINR threshold increases *CTXability*	5.4.2
Tx Power control increases *CTXablity*	5.4.3
Quantification of CTXability: Uncontrollable parameters	
Effect of Path loss exponent on *CTXability* is dependent on location and power flexibility	5.5.1
CTXable links are prevalent in real-world	5.5.2
Concurrent transmission is at least *capturable* in general	5.6
Experiments with MicaZ motes validate simulation results	6

Table 1. Contributions of this paper

1 Introduction

Concurrent packet transmission has been considered harmful and avoided in wireless communication. Protocols such as 802.11 explicitly prevent concurrent transmission with carrier sensing and by exchanging RTS/CTS messages (as proposed earlier [2]). Nevertheless, *concurrent communication*—allowing concurrent transmission by two senders over the same channel—can be beneficial if both receivers can concurrently receive what is sent. Approaches such as RTS/CTS handshake reduce multi-hop wireless throughput by blocking all other transmission around both the sender and receiver. Concurrent communication could greatly improve throughput, particularly when traffic is heavy and network density is high.

The possibility and promise of concurrent packet transmission has recently been demonstrated in several studies [6, 7, 14, 16, 18]. The benefits of concurrent communication seem obvious, when it is possible, because it will improve spatial reuse, resulting in higher throughput. However, it is not obvious that how often concurrent transmission is possible. For example, if one pair of nodes always transmits at the lowest power level possible, then any other concurrent transmissions will increase the effective noise and force the original pair to raise its power. This coupling may

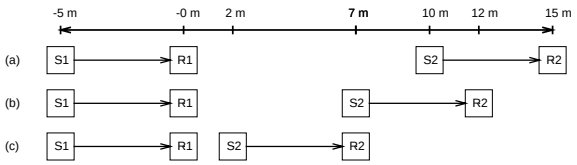

Figure 1. Two concurrent packet communications at three different locations

mean that there is never a significant benefit to concurrent transmission.

To illustrate this question, Figure 1 shows three configurations where two pairs of nodes send concurrently, S1 to R1 and S2 to R2. We assume a nominal radio range of 8 m at -10 dBm transmission power. In case (a), the pairs are 10 m apart and can easily send concurrently, even with an RTS/CTS-based MAC protocol, since nodes are out of range of each other. On the other hand, in case (c), R1 and S2 are only 2 m apart, and no attempt at concurrent transmission will be successful. Although S1's transmission can be received at R1, if S2 attempts to send concurrently, S1 must raise its power due to interference from S2, and this higher power forces S2 to raise *its* power, ad infinitum. However, there are intermediate cases where concurrent transmission is possible (as suggested in [16]). For example, when the R1-S2 distance is 7 m as in case (b), then 802.11's RTS or CTS will block concurrent transmission. However, with proper MAC support both S1 and S2 can simultaneously capture the channel at its corresponding receiver. We look at this example and others in more detail in this paper.

Table 1 summarizes the contributions of this paper. First, we develop a simple decision rule to decide when concurrent communication is possible while minimizing transmission power. With this decision rule, we can determine if concurrent transmission is ever possible for a given topology, and then compute the optimal (minimal) transmission power settings for successful concurrent communication, if possible.

Through simulations, we then systematically quantify opportunities for concurrent communication with and without transmission power control as many radio and environmental parameters vary, including node position, mean and variance of path loss, signal-to-interference-plus-noise-ratio (SINR) threshold, and granularity and range of transmission power control.

We also introduce and use a new metric to estimate the feasibility and benefits from allowing concurrent transmission for different environmental and hardware conditions. Our simulations show that often, 40–75% of the time, depending primarily on distance and location, two pairs of nodes can communicate concurrently. We can observe large CTXable region even with fixed transmission power, but dynamic power control significantly improves concurrent communications. We validate key results through experiments over MicaZ motes with 802.15.4 radios, confirming concurrent transmission is possible and validating our simulation results.

2 Related Work

A great deal of prior work has empirically studied low-power wireless transmission [1, 4, 5, 8, 15, 17, 19, 20, 21, 22, 24]. This work has improved our understanding of the wireless communication and also provides better communication models and metrics. However, these studies do not consider the situation where multiple senders transmit packets simultaneously. In fact, a design goal of most current media-access protocols is to avoid concurrent transmissions, often within a two-hop neighborhood of the sender.

Recent work has begun to relax this assumption and explore the implications of concurrent transmission [6, 7, 14, 16, 18, 23]. In densely deployed wireless sensor networks, concurrent packet transmission is endemic. Whitehouse et al. [18] and Son et al. [16] were the first to systematically explore the effects of interference and concurrent transmission, in Mica2 and MicaZ motes. However, unlike our focus here, they both study the case where multiple transmitters send to a common receiver. Thorough experimental study provides useful guidelines to interference-aware protocol design and demonstrates the feasibility of concurrent communication. Reis et al. introduce two physical layer models that provide effective prediction of the probability of packet delivery under interference from concurrent transmission [14]. These models are based on the RF measurements from real 802.11 testbed. Recently, Moscibroda et al. analytically and empirically study the inaccuracy and inefficiency of protocol design based on graph-based model [11], and analyze the capacity of wireless network with a physical model allowing concurrent communications [10].

Transmission power control plays a key role in interference-aware protocol design by controlling the intensity of the signal and interference strength. Even though there have been extensive research efforts with transmission power control in wireless communication, there are few *empirical* studies that consider transmission power control. Son et al. [15] study the effects of transmission power control on wireless link quality on real sensor network testbed with Mica2 motes. They propose a power control scheme with link blacklisting to improve link reliability and energy efficiency. Recently Lin et al. [9] proposed an adaptive transmission power control (ATPC) protocol based on the empirical measurements from the MicaZ motes with 802.15.4 radios [3] which reacts to the temporal change of the link quality with explicit on-demand feedback packets. However, both these works do not explicitly study the benefits from transmission power control for concurrent packet communication.

3 Motivating Example

We define two (or more) transmissions as *concurrently transmittable* or *CTXable* if they can both successfully be received at the same time. Traditional MAC protocols such as 802.11 ensure collision-free packet communication by carrier sensing followed by RTS/CTS handshakes that bar communication from nodes within one hop of either the sender or receiver, while other protocols (for example, TRAMA [12]) adopt a TDMA-based schedule with two-hop neighbors in mind. In this paper, we explore the use of channel capture

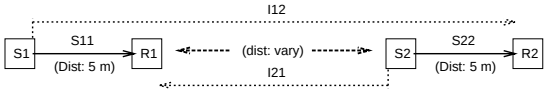

Figure 2. Example scenario with two concurrent packet sender-receiver pairs varying R1-S2 distance. $PL_0 = 45$**,** $n = 4$**,** $SINR_\theta = 4$**,** $X_\sigma = 0$**,** $N_1 = N_2 = -95\ dBm$**, Fixed Tx power**$= -10\ dBm$

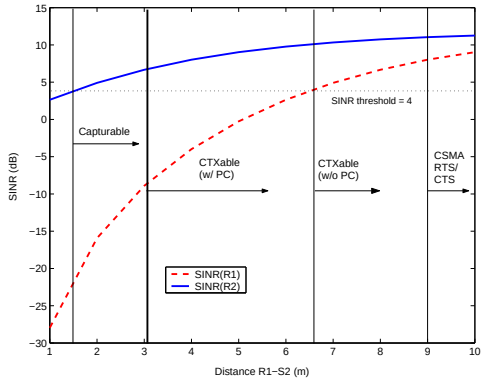

Figure 3. CTXability for different schemes. SINR values are measured at -10 dBm fixed Tx power

and transmission power selection to allow CTXable communication when nodes are within range of each other.

In this section we explore how transmission power and node location interacts to allow CTXable communication in some cases. To introduce CTXable communication we first use simulation to explore how transmission power and source and destination location affects the ability to communicate.

Figure 1 showed several scenarios where both senders (S1 and S2) concurrently transmit packets to their corresponding receivers (R1 and R2). We generalize this example with variable distance between R1 and S2 in Figure 2. We denote the signal strength from sender i to receiver j as S_{ij}, and the interference it generates at the other receiver k as I_{ik}. We define ambient noise at each receiver as N_j. Throughout this simulation, we use the same link distance of 5 m between each sender and receiver. Under the constant radio and environmental parameter settings (presented in the caption of Figure 1, we only vary the distance between the R1 and S2 and calculate signal and interference value based on an *exponential path loss model* (details of this model are explained in Section 4). We consider the SINR value greater than equal to 4 as a threshold for successful communication (i.e., $SINR_\theta = 4$) in this simulation. We consider the signals arrived from unintended senders as interference in SINR calculation at each receiver.

Figure 3 shows simulations as the S2-R2 pair of nodes moves right and left. We compare the distance from R1 to S2 against the SINR values of the intended transmissions when both senders transmit at a power of -10 dBm. At this transmission power, either communication would succeed if it occurred separately, but here we can identify four different regions of communication when both senders transmit at the same time.

Starting at the right of the figure, when R1-S2 is 9 m or further away, we call this the *CSMA RTS/CTS CTXable region*. Intuitively, at these distances, nodes just cannot hear each other and so spatial reuse allows them to operate independently. With MAC protocols such as 802.11, carrier sensing and RTS/CTS handshake are used to prevent concurrent transmission. The *carrier sense threshold* is always set to less than equal value to the RSS which ensures successful packet reception. We use the received signal strength (RSS) of -91 dBm as a *packet reception threshold* in our simulation (based on the empirical results with MicaZ mote). We also choose the same RSS value as packet reception threshold as the carrier sense threshold, which is the maximum plausible value in this example. With lower carrier sense threshold (which is more general setup in conservative 802.11 MAC), the *802.11 CTX region* becomes smaller. In other words, longer than 9 m link distance between R1-S2 is required for 802.11 CTX in real implementations.

We call the next region from the right, when R1-S2 is just less than 7 m to 9 m, *CTXable* without transmission power control. Concurrent communication is possible in this region at constant transmission power because both receivers can capture the intended packet, since both have a higher SINR value than $SINR_\theta$ at the given default transmission power.

Next, we see that with transmission power control, there is an even more expanded CTXable region starting from about 3 m. We will show how to select the power appropriately to enable CTX in this region, in the next section. The combined region from 3 m to 9 m thus represents the zone where a sophisticated MAC could allow communication that would be prevented by MACs that use CSMA and RTS/CTS, similar to 802.11.

The next region, with R1-S2 distance starting at about 1.5 m, is a case where one sender (in this case S2) can capture the channel, but the other sender cannot communicate successfully (only one receiver's SINR exceeds $SINR_\theta$). We define this region as *capturable region*.

Finally, in the leftmost region, where R1-R2 is less than 1.5 m, neither pair can communicate. The receivers are located too close together and neither can capture the channel. Both receivers have SINR values lower than $SINR_\theta$ and their transmissions will always collide and corrupt each other. In this region, both senders need to increase their transmission powers to meet the $SINR_\theta$ condition for successful communication. But, if one sender attempts to increase its transmission power to capture the channel, this further increases the interference at the other receiver. The other sender requires to increase its transmission power to overcome this extra interference and it only neutralizes the benefits from the transmission power control. Therefore, CTX is never possible even with transmission power control in this region.

These different regions suggest the complex interaction between concurrent senders. We next define and model concurrent communication more formally.

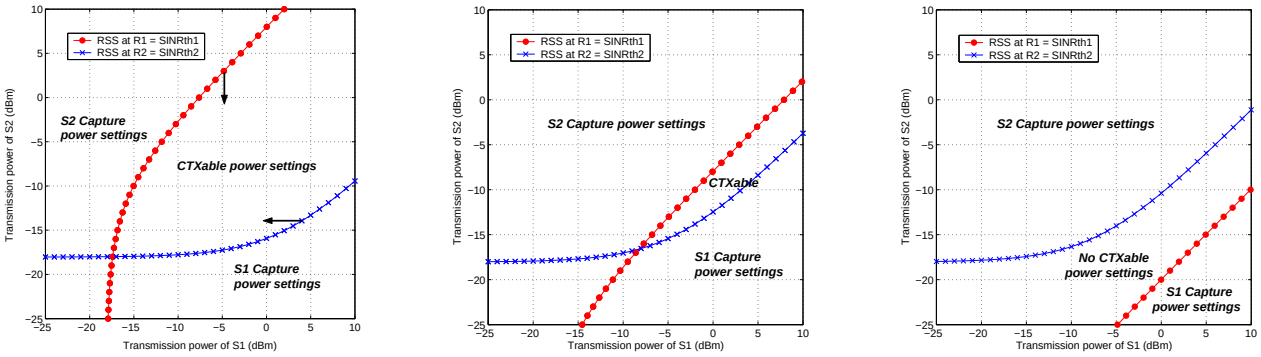

(a) $d_{R1-S2} = 10\,m$, $lf_1 = 4$, $lf_2 = 2$ (b) $d_{R1-S2} = 4\,m$, $lf_1 = 1.8$, $lf_2 = 0.8$ (c) $d_{R1-S2} = 2\,m$, $lf_1 = 1.4$, $lf_2 = 0.4$

Figure 4. The CTXable transmission power relationship between S1 and S2. $PL_0 = 45$, $n = 4$, $SINR_\theta = 4$, $X_\sigma = 0$

4 Mathematical Modeling

We begin by modeling mathematically when concurrent transmissions can occur for the case of two senders and two receivers. For our modeling, we use the *exponential path loss model with log-normal fading* [13, 24]:

$$\begin{aligned} PL(d)_{dB} &= PL(d_0)_{dBm} + 10n\log(d/d_0) + X_{\sigma_{dB}} \quad (1) \\ P_r(d)_{dBm} &= P_{t_{dBm}} - PL(d)_{dB} \end{aligned}$$

Here P_t and P_r are the transmission and reception power in dBm. The sender-receiver distance is d, and d_0 is the reference distance for path loss *(PL)*. X_σ is the variance in path loss due to multipath fading, modeled as Gaussian random variable with zero mean and standard deviation σ_{dB}. This model defines the path loss and the received signal strength (RSS) at the receiver for a given transmission power level.

4.1 Power setting for CTXability

For concurrent transmission to be possible, the received SINR must be above the threshold for each receiver ($SINR_{\theta r}$ for receiver r):

$$\begin{aligned} S_{11_{dBm}} - 10\log(10^{I_{21_{dBm}}/10} + 10^{N_{1_{dBm}}/10}) &\geq SINR_{\theta 1_{dB}} \quad (2) \\ S_{22_{dBm}} - 10\log(10^{I_{12_{dBm}}/10} + 10^{N_{2_{dBm}}/10}) &\geq SINR_{\theta 2_{dB}} \end{aligned}$$

For a given distance-based path loss model, such as the one we described in Equation 1, we get the following non-linear inequalities relating the transmission powers of both senders, given a sender x to receiver y distance of d_{xy} and transmission power of $P_t(s)$ for sender s:

$$\begin{aligned} P_t(S1) &\geq PL(d_{11}) + SINR_{\theta 1} + \quad (3) \\ &\quad 10\log(10^{(P_t(S2)-PL(d_{21}))/10} + 10^{N_1/10}) \\ P_t(S2) &\geq PL(d_{22}) + SINR_{\theta 2} + \\ &\quad 10\log(10^{(P_t(S1)-PL(d_{12}))/10} + 10^{N_2/10}) \end{aligned}$$

We can visualize these non-linear inequalities as regions in a plot where the axes represent the transmission powers $P_t(S1)$ and $P_t(S2)$. The intersection of regions would then indicate when both conditions are satisfied simultaneously, i.e. when concurrent transmissions are possible. From the above equation, we see that the shape of these regions would be primarily determined by the path loss model and the inter-node distances. Figure 4 shows these regions for three different node topologies.

Figure 4(a) shows regions corresponding to the non-linear inequalities for the scenario shown in Figure 2 at 10 m of R1-S2 distance. Each line indicates the sender's optimal transmission power which meets the SINR threshold requirement at its intended receiver with equality. The line with circles shows calculated S1's optimal transmission powers if the S2's transmission power varies between -25 and 10 dBm as shown in the Y-axis. The region to the bottom-right of this curve represents all combinations of transmission powers that allow receiver R1 to capture the message. The line with crosses similarly shows S2's calculated optimal powers for different S1's transmission power selections. The region to the top-left of this curve shows all combinations of transmit powers that allow receiver R2 to capture the message. The overlapping region, therefore, shows the combination of transmission powers that allow for concurrent transmission (i.e., these are the CTXable power settings).

As shown in the plots in Figure 4, the extent and the existence of the overlapping CTXable region depends upon the inter-node distances. In particular, compared to (a), (b) shows a smaller CTXable region requiring higher transmit powers as the R1-S2 distance becomes smaller; when the R1-S2 distance is reduced even further in (c), we find that the two regions no longer overlap.

The crossing point of the two lines in Figure 4 provides the optimal S1 and S2's transmission power combination, which is the minimum transmission power setting for CTX. We can actually solve analytically for this crossing point (when it is possible) by treating the inequalities from Equation 3 as simultaneous non-linear equations. This yields the following expressions for the *optimal transmission power*

settings for S1 and S2:

$$P_t(S1) = PL(d_{11}) + SINR_{\theta 1} + 10\log(10^{(P_t(S2)-PL(d_{21})/10} + 10^{N_1/10}) \quad (4)$$

$$P_t(S2) = 10\log(10^{(PL(d_{11})-PL(d_{12})+SINR_{\theta 1}+N_1)/10} + 10^{N_2/10}) - 10\log(10^{-(SINR_{\theta 2}+PL(d_{22}))/10} - 10^{(PL(d_{11})-PL(d_{12})-PL(d_{21})+SINR_{\theta 1})/10})$$

Equation 4 provides the optimal transmission power to use for each sender S1 and S2 without exhaustive trial and error. Optimal power setting consumes minimum energy for concurrent communication causing minimal interference to the network.

4.2 Topology Condition for CTX

We can get some analytical insight into the impact of topology by deriving a necessary and sufficient condition for CTXability. In order to ensure that the simultaneous non-linear equations have a bounded solution, it can be shown that the following topology condition is necessary and sufficient (this condition ensures that the logarithm in equation 4 has a positive argument):

$$SINR_{\theta 1} + SINR_{\theta 2} < PL(d_{12}) - PL(d_{11}) + PL(d_{21}) - PL(d_{22}) \quad (5)$$

Adopting the exponential path loss model from Equation 1, this can be written as:

$$SINR_{\theta 1} + SINR_{\theta 2} < 10n(\log(\frac{d_{12}}{d_{11}}) + \log(\frac{d_{21}}{d_{22}})) \quad (6)$$

Let us define the *location flexibility* lf_i for each sender i as the ratio of the distance between a sender and its intended receiver to the distance between a sender and its unintended receiver (i.e., interfered node). Thus $lf_1 = \frac{d_{12}}{d_{11}}$ and $lf_2 = \frac{d_{21}}{d_{22}}$. The *lf* value indicates the endurance level to the additional interference and noise under concurrent transmission. Depending on the *lf* value of each sender (the higher the better), the possibility of CTX and the area of the CTXable second sender location changes. This can be seen in Figure 4.

4.3 CTXability with limited power range

We have now shown how to determine optimal transmission power for concurrent transmission: evaluate the topology condition to determine if CTXability is possible (Equation 5, and if so, compute the optimal transmission powers with Equation 4). Real hardware, however, has limited control over transmission power in terms of supported range and granularity. If the optimal power computed above is supported, we are done. If not, we next consider *how to adapt to constrained choice of power settings*:

If either optimal transmission power level is greater than that supported by the hardware, CTX is not possible.

If either one of the optimal transmission powers is lower than supported power range, we set the transmission power of this node to the minimum supported transmission power for that node and calculate the transmission power of the other sender with Equation 4. CTX is possible only if the calculated transmission power is within the supported power range.

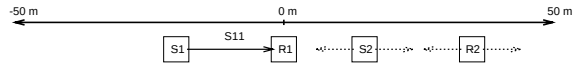

Figure 5. Simulation topology: two sender-receiver pairs

If both selected transmission powers are below the supported minimum power levels, we select the one with higher difference between the optimal transmission power and its minimum supported power (let's call this first sender). It attempts to send at its minimum supported power level, and we compute the other required transmission power accordingly. If this exceeds its range, CTX is not possible. Otherwise we use the suggested power for the second sender, or bring it to the minimal supported range if it was lower than what is supported. This is because the increase of the second sender's transmission power level to its minimum supported power range is still less than the increase of the first node's transmission power. Therefore, the first sender can tolerate the increase of the second sender's transmission power level.

The basic rule is that the increase of the same amount of transmission power for both CTXable senders from the CTXable power level always allows CTX at their new transmission power level, if new power levels are supported. This is because the effect from the noise decrease at higher transmission power or higher received power level. Therefore, the same amount of signal and interference increase always ends up with higher SINR at the receiver.

4.4 Summary

To summarize, the following are the two controllable factors that play an important role in CTXability. First, CTXability depends on the *location flexibility*. Higher *location flexibility* increases the possibility of CTX, represented by a greater gap between the two lines in S1 and S2's optimal power plot. Second, CTXability depends on the transmission *power flexibility*, which means the range of controllable transmission power (i.e., the minimum and maximum transmission power level). Higher transmission power flexibility improves the CTXability by increasing the chance of meeting the required CTXable transmission power for each sender. Therefore, we can expect higher CTXability from higher *flexibility* from location and transmission power range.

5 Simulation

In this section we analyze the feasibility of concurrent packet transmission through systematic simulations to understand the effects of user controllable and radio parameters such as node position, SINR threshold ($SINR_\theta$), range and granularity of transmission power control), and uncontrollable and environmental parameters like path loss exponent (n), and the variance in path loss due to multipath fading (X_σ) on CTXability.

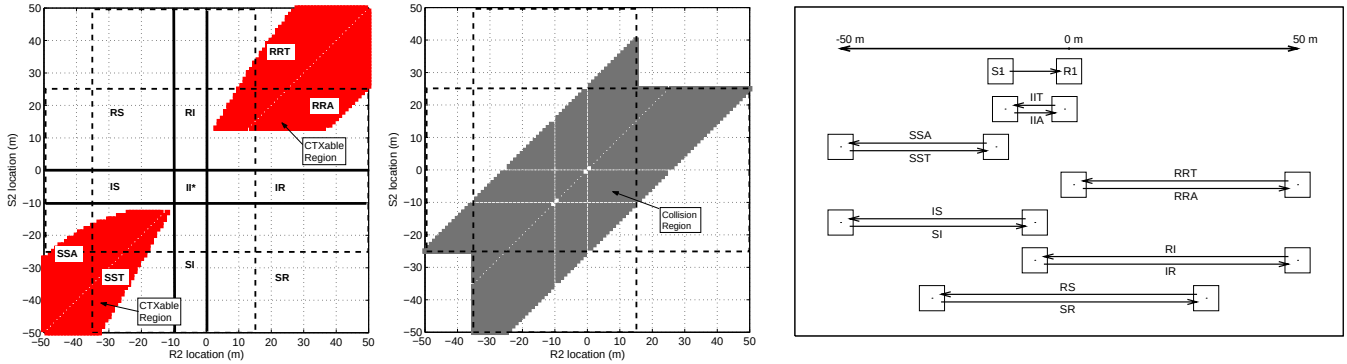

(a) Area index (b) Collision Region (c) Example for each area index

Figure 6. Simulation result example with area index: fixed transmission power of 10 dBm for (a) and (b). $S1,R1 = (-10,0)$**,** $n = 4$**,** $SINR_\theta = 4$**,** $X_\sigma = 0$

5.1 Methodology

When we simulate a specific topology for a CTXability test, the main variable parameter of interest is the relative positions of the *senders and receivers*, rather than exact node locations. To make exploration of the topology space manageable, we consider only four nodes (two senders and two receivers) and place them on a line over 100 m as shown in Figure 5. Even with this simple line topology we can test large number of distance combinations; we will consider more general 2D topologies in our future work. To characterize the topology we name the two sender-receiver pairs S1-R1 and S2-R2. We define the origin of the line as the location of the receiver R1. In each simulation we position S1 and R1 and then vary the locations of S2 and R2, testing for CTXability. We typically fix other parameters (S1-R1 distance, transmission power, and noise) then plot CTXability as a function of locations of S2 and R2, showing the minimum required transmission power of either S1 or S2 for concurrent communication.

Our tested CTX related parameter values change for different hardware (especially radio, antenna) and environmental conditions. Because there are many parameters to explore, we generally hold all fixed but one for each section. We always use ambient noise N of -95 dBm and path loss at reference distance $PL(d_0) = -35$, and the following is the most common setup for other parameters: path loss exponent $n = 4$, $SINR_\theta = 4$ dB, $X_\sigma = 0$ dB. Our radios are modeled on the Chipcon CC2420 RF transceiver, an 802.15.4 radio widely deployed in the MicaZ and Telos-B motes. When we consider controllable transmission power, we normally limit them between -25 dBm and 0 dBm as with this radio.

5.2 Defining Regions of Placement and the CTXable Ratio

To simplify discussion, we begin by presenting an example and showing potential relative placement of the two pairs of nodes. Figure 6(a) shows one set of simulation results. In this paper, we list the locations of sender and receiver in order in parentheses (in meters on the line) followed by sender and receiver id. This figure shows a sample simulation result when both senders use a fixed transmission power level of 0 dBm and $S1,R1 = (-4,0)$. X-axis shows the R2 location in meters and Y-axis shows the S2 location. S1 and R1 locations are fixed for each simulation set.

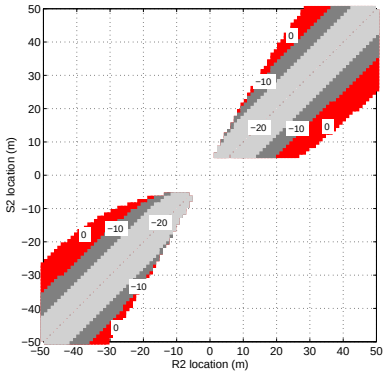

Figure 7. CTXable regions with different fixed transmission power levels. $S1,R1 = (-4,0)$**,** $n = 4$**,** $SINR_\theta = 4$**,** $X_\sigma = 0$

To compare CTXability with an RTS/CTS-based protocol we bound the nominal communication range (without collision) with horizontal and vertical lines. Vertical lines indicate the one-hop area around R1 that would be blocked by its CTS, and horizontal lines show the same region around R2. We define *collision region* as the region where concurrent packet transmission is prohibited by RTS/CTS-based protocol to avoid packet collision. Each sender only transmits a packet when its intended receiver is located within its communication range. Therefore, the actual collision region is smaller than the whole areas within two vertical and horizontal lines. Figure 6(b) shows an example of traditional collision region when $S1,R1 = (-4,0)$. For each simulation S1 and R1 locations are constant and the collision area is set based on these static node locations.

Figure 6(a) shows two dark CTXable regions. These regions let us quantify the benefits of CTXability. We define *CTXable ratio* as *CTXable region* within *collision region*.

$$CTXable ratio = CTXable\ region\ /\ Collision\ region$$

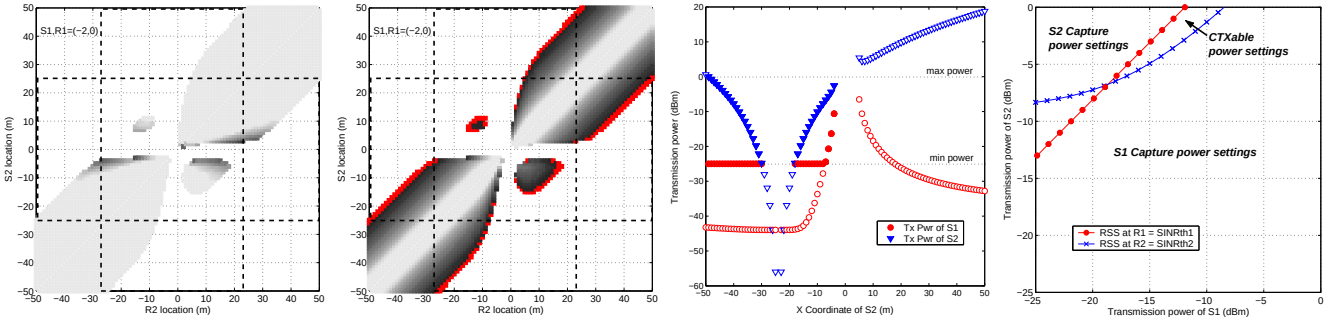

(a) Optimal Tx Power of S1 (b) Optimal Tx Power of S2 (c) Optimal Power Settings (d) CTXable Power Settings

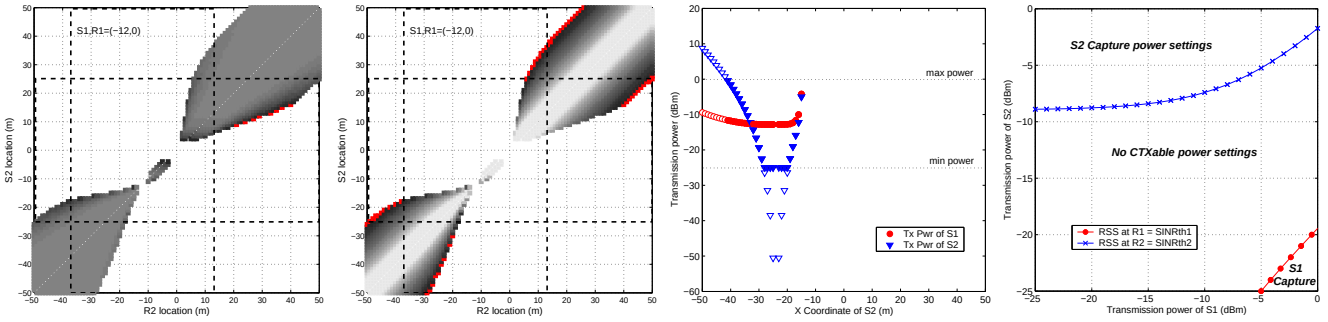

(e) Optimal Tx Power of S1 (f) Optimal Tx Power of S2 (g) Optimal Power Settings (h) CTXable Power Settings

Figure 8. CTXable regions and optimal Tx Power for S1 and S2 varying distance: $S1,R1 = (-2,0)$ *for* $(a)-(d)$, $S1,R1 = (-12,0)$ *for* $(e)-(h)$, $n = 4$, $SINR_\theta = 4$, $X_\sigma = 0$, $S2,R2 = (-5,10)$ *for* (d) *and* (h)

This ratio reflects the fraction of area where a MAC protocol that supports concurrent transmission can send when a traditional MAC protocol would prohibit concurrent communication. A larger CTXable ratio potentially allows greater overall network throughput and more spatial reuse.

Next, to explain why these regions are CTXable, Figure 6(c) shows twelve different configurations of S2 and R2 relative to S1 and R1, and labels each with a three letter code. The first two letters of each code indicate the location of S2 and R2 relative to S1-R1: I means inside S1-R1, S means outside S1-R1 on S1 side, R means outside S1-R1 on R1 side. We use the third character to indicates the direction of the S2-R2 communication, if necessary: A is away from S1, T is towards S1, or * is either.

Returning to Figure 6(a), we see that the regions which are CTXable are typically RR* or and SS*, where S2-R2 are on either side of S1-R1. They must be far enough away not to interfere: CTX is possible when S2-R2 are at 7 m and 12 m, and fails when they are at 2 m and 7 m. These are similar cases as Figure 1(b) and (c). However, here we can see all possible combinations of distance for successful concurrent packet communication. We broaden this discussion as we go to consider other parameter settings and node locations.

5.3 Fixed Transmission Power Cases

Many protocols are designed assuming that nodes always transmit at the same power, because some radios do not support and protocols do not exploit power control. We consider fixed transmission power here, and generalize to controllable power in the next section.

Figure 7 shows CTXability as S2 and R2 move for three

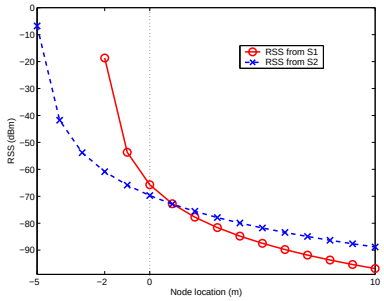

Figure 9. Comparison of RSS from S1 and S2. $S1,R1 = (-2,0)$, $S2,R2 = (-5,10)$, $n = 4$, $SINR_\theta = 4$, $X_\sigma = 0$

fixed transmission power levels of -20, -10, and 0 dBm. We hold all other parameters constant as the caption shows. This figure shows that the CTXable region is larger at higher transmission powers. As transmission power grows from -20 to 0 dBm, we see the CTXable ratio grow from 0.26 to 0.44.

The CTXable ratio grows for larger powers because the higher interference from stronger transmission is more than offset by the increased signal strength. In addition, the larger transmission power increases the size of collision region that would be reserved with an RTS/CTS protocol. Considering node placement (defined in Figure 6(c)), with fixed transmission power we only see CTXability in the RR* and SS* regions (we will later show that power control allows CTXability elsewhere). This limitation is because the flexibility

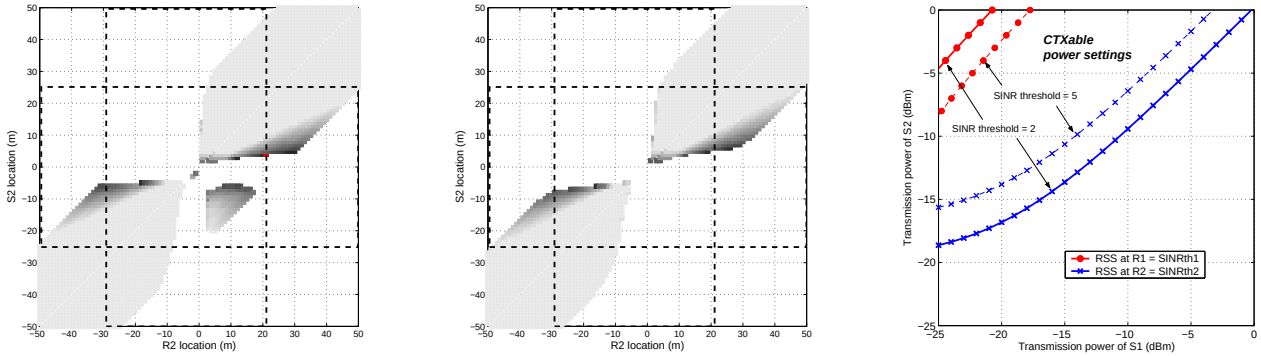

(a) $SINR_\theta$=2 (b) $SINR_\theta$=5 (c) CTXable Power Settings

Figure 10. CTXable regions with different $SINR_\theta$: $S1, R1 = (-4,0)$, $n = 4$, $X_\sigma = 0$, $S2, R2 = (15,6)$ *for* (c)

is limited when transmission power is fixed — there is no *power flexibility* — so communication distance is the only factor that contributes the signal and interference strength. Therefore, the sender always needs to be located closer than the interferer for every receiver to have a positive SINR value which meets the intended receiver's SINR threshold.

With fixed power, communication is only CTXable when these conditions hold:

$$SINR_{\theta 1} \leq 10n\log\left(\frac{d_{12}}{d_{11}}\right) = 10n\log(lf_1) \qquad (7)$$

$$SINR_{\theta 2} \leq 10n\log\left(\frac{d_{21}}{d_{22}}\right) = 10n\log(lf_2)$$

As this condition implies, the leftover SINR value (i.e., signal strength) for each communication cannot be used to increase the CTXability in fixed power case; while we can adjust SINR values between two receivers with distinct transmission power settings for each sender (i.e., with power control) to improve CTXability.

5.4 User Controllable Parameters

Users can control some aspects of their network, including their location and their choice of radio. We next consider CTXability when we vary these parameters.

5.4.1 Location change

One of the most important parameters is node location. An important design consideration of any sensornet deployment is how many nodes will be deployed and where. With stationary nodes, particular locations will allow or preclude CTXability; when nodes moving or are randomly positioned, we can at least characterize the probability of concurrent communication. To systematically explore the effect of node location we fix R1 at 0 m and move the other nodes. For a given experiment we typically fix S1 (and so the S1-R1 distance), then test all combinations of S2-R2 placement.

Figure 8 presents CTXable regions and optimal S1 and S2 transmission powers settings for two different S1-R1 distances of 2 m (top row) and 12 m (bottom row). Transmission power is shown as grayscale on the right and center graphs (darker values indicate greater transmission power, red is the darkest indicating the maximum power), and called out specifically for one S2, R2 case in the rightmost graphs (8(d) and 8(h)).

In general, S1's optimal transmission power is stable (Figures 8(a) and 8(e)) because neither S1 nor R1 move in these simulations. However, there are some locations where interference from S2 forces S1 to increase its transmission power: darker region in Figure 8(a), for example, $S2, R2 = (4,27)$. S2's transmission power spans a much larger range (Figures 8(b) and 8(f)), mainly due to changes in the S2-R2 distance. These figures show considerable amount of CTXable region inside the collision region: CTXable ratio values are 0.77 for an S1-R1 distance of 2 m and 0.43 for 12 m. Greater CTXability is possible when S1 and R1 are closer because they can communicate at lower power. In other words, longer distances imply higher interference and lower location flexibility for CTX.

Figure 8(c) and 8(g) show the S1 and S2's optimal transmission power setting for concurrent transmission both when we relax the power control limitation (shown in filled symbols) and when we have -25 *dBm* and 0 *dBm* constrained power range (shown in empty symbols). First these figures presents the optimal power change due to hardware limitation. We can also see that at higher S1-R1 link distance of 12 m, optimal transmission power (noticeably for S1) increases. This is because of the worse location flexibility for S1. Lower flexibility means reduced chance of concurrent transmission under the same condition. We can see that CTXability is greatly reduced at longer distance (in Figure 8(h)).

Finally, when we compare CTXable region in Figure 8 to fixed power (Figure 6), we see that concurrent communication is sometimes possible in the *SR* or *RS* regions with power control. This means that S2 and R2 are on *opposite sides* of S1-R1—sometimes S2-R2 can transmit *over the heads* of S1-R1! If S2 selects an appropriate transmission power which only increases the interference, but does not corrupt the packet from S1, while S2 can still provide strong enough signal strength for a packet reception at R2. This becomes possible with a proper transmission power setting for each sender. Figure 9 compares the RSS from each sender at different node location under the same *SR* scenario presented in Figure 8(d), and using the optimal transmission power

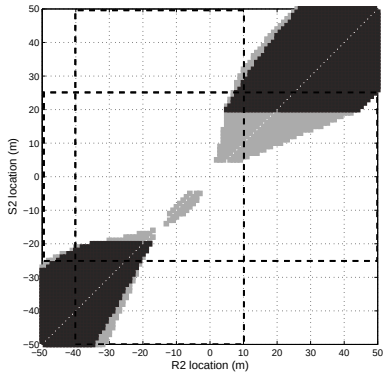

Figure 11. CTXable region comparison with and without power control. $S1, R1 = (-15, 0)$**,** $n = 4$**,** $SINR_\theta = 4$**,** $X_\sigma = 0$

shown in this figure: -18.67 *dBm* for S1 and -6.77 *dBm* for S2. In this case, both R1 (at 0 m) and R2 (at 10 m) receive stronger signal strength from its intended sender, also meeting SINR threshold of 2 *dB*. This figure visually explains how concurrent communication is possible for this unlikely situation with transmission power control.

5.4.2 SINR threshold

A recent work has shown that different hardware requires different signal-to-interference-plus-noise ratios ($SINR_\theta$) to reliably send data [16]. In this section, we want study the effects of $SINR_\theta$ on CTXability.

Figure 10 shows the CTXable region and CTXable transmission power range for two different $SINR_\theta$ values of 2 and 5 (fixing S1 and R1 and -4 m and 0 m). We see that a larger $SINR_\theta$ value reduces the CTXable region. A larger $SINR_\theta$ reduces the power flexibility of both senders, since each must have greater "headroom" to successfully communicate (due to the summation of SINR thresholds in Equation 6 as shown in Figure 10(c)). The CTXable ratio of these cases are 0.75 and 0.61 for $SINR_\theta$ of 2 and 5 respectively, so this loss of flexibility translates into 14% less opportunity for CTXable communication for this specific case.

The effect of SINR threshold value changes under different communication environments. When we reduce the path loss exponent from 4 to 3, the CTXable ratio difference increases to 0.25 (0.77 and 0.52 for $SINR_\theta$ of 2 and 5 respectively). Lower n value decreases the signal strength difference at the same link distance and the link distance between the sender and interferer need to be greater for the same $SINR_\theta$. In other words, the same SINR gap (or *location flexibility*) covers larger distance (or region). Therefore, SINR threshold plays more significant role under lower n value situation. This simulation shows that the impact of SINR threshold change (due to hardware differences) cannot be ignorable, and it varies under different environmental conditions.

5.4.3 Comparing Fixed and Dynamic Power Control

Now that we understand the effect of node location, we next quantify the advantage of dynamic power control over fixed transmission power. To do so we compare the relative sizes of CTXable region with and without power control at three different S1-R1 distances: 5 m, 10 m, and 15 m.

Figure 11 compares the CTXable region with fixed power control (the dark gray regions) with the additional area added with dynamic power control (the light gray regions) when the S1-R1 distance is 15 m. For the fixed-power case S1 sends at the maximum transmission power of 0 dBm, since this provides the largest CTXable region (Section 5.3). In this case the CTXable ratio is 0.22 without power control and 0.36 with power control; when the S1-R1 distances are 5 m and 10 m we see similar tendencies (fixed vs. dynamic CTXable regions of 0.42 vs. 0.63 at 5 m and 0.33 vs. 0.48 for 5 m and 10 m, respective).

From this comparison and the simulation results presented in previous sections, we conclude that power control provides significantly greater CTXability than fixed power control for a given topology. The CTXable region difference with and without power control becomes greater when the S1-R1 distance is greater the location flexibility becomes much worse at longer link distance, and the fixed power scheme cannot overcome this because it does not have any *power flexibility* like dynamic power control case.

5.4.4 Power control granularity

We have also simulated the effects of the granularity of transmission power control. The Chipcon CC1000 supports transmission power levels between -20 dBm and 10 dBm, selectable at 1 dBm increments across most of this range. The newer Chipcon CC2420 provides a similar range (from -25 dBm to 0 dBm), but it support only 8 distinct settings over this range (-25,-15,-10,-7, -5,-3,-1, and 0 dBm).

We compare the simulation results between the case with 8 levels and 25 levels of finer transmission power control at the same -25 *dBm* to 0 *dBm* power range. Finer level of transmission power control slightly increases CTXable region (about 3% in CTXable ratio) with more possible transmission power combinations in general, and it also lowers the transmission power for some CTXable locations. Therefore, we can expect some minor benefits to the CTXability and energy consumption with finer transmission power control.

5.5 Uncontrollable and Environmental Parameters

While some parameters are under user control, wireless propagation itself is known to be highly variable and unpredictable. We next consider CTXability as we vary path loss exponent and path loss variance from the exponential path loss model with log-normal fading (presented in Equation 1).

It is well known that this model only approximates wireless propagation, so we supplement these results with testbed experiment in Section 6.

*5.5.1 Path loss exponent (*n*)*

Propagation environment distinguishes received signal strength and quality for the same hardware at different node locations in wireless communication. The path loss exponent n is a primary parameter that determines signal strength in different communication environments. According to the prior study [13], different environments are modeled by path-loss exponents from 1.6 to 6. A larger n increases the path loss, decreasing the viable reception distance and, for a given

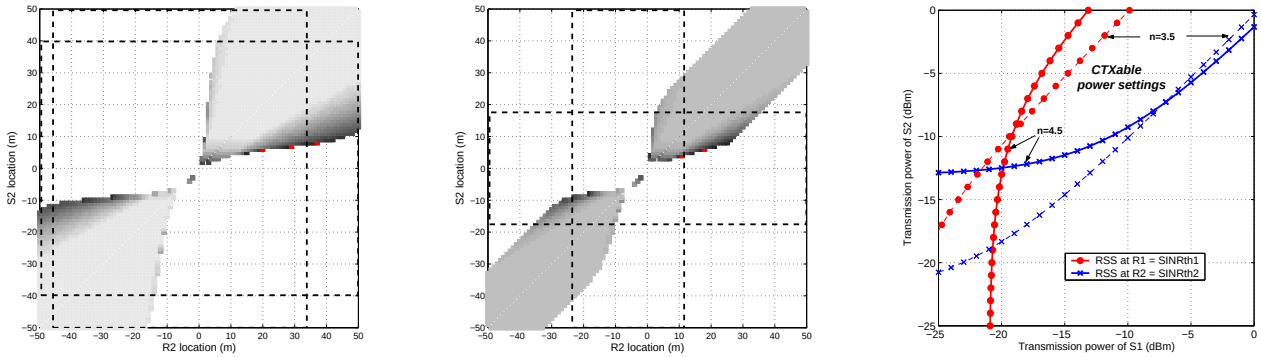

(a) n=3.5 (b) n=4.5 (c) CTXable Power Settings

Figure 12. CTXable regions with different path loss exponent. $S1, R1 = (-6, 0)$**,** $SINR_\theta = 4$**,** $S2, R2 = (15, 6)$ **for (c)**

distance, decreasing the received signal strength and interference.

Figures 12(a) and 12(b) compare CTXability with path loss exponents (n) of 3.5 and 4.5. Note that the lower n corresponds to a larger effective transmission range, as shown by the dashed line box indicating the collision region. When we compare Figure 12(a) with Figure 12(b), we can clearly see the difference in CTXable location between these two cases, but not in the CTXable ratio value. We observe the same CTXable ratio of 0.56 from both cases with different path loss exponent of 3.5 and 4.5.

When we compare the possible transmission power combination in 12(c), we can see the higher n value increases the minimum transmission power for CTX (transmission power for S1 and S2 respectively changes from -26.8 dBm and -21.3 dBm to -19.9 dBm and -12.4 dBm) because it reduces the communication range at the same transmission power level, but higher n value also increases the possibility for CTX by increasing the effect of location flexibility in right side of Equation 6.

Even though higher n value can increase CTXable region (according to Equation 6), this advantage comes together with higher transmission power requirement for CTX at the same topology. Therefore, higher path loss exponent can increases CTXable region only when it supports increased transmission power requirement. However, transmission power range is very limited especially with low-power wireless networks in general.

On the contrary, lower n value decrease the minimum transmission power required for CTX, but if the path loss exponent value becomes too low, it greatly reduces the location flexibility (i.e., distance effect), and this can make CTXable two communications (at higher n) non-CTXable. Therefore, the relationship between the path loss exponent and CTXability varies depends on the given location and power flexibility.

5.5.2 *Path loss variance:* X_σ

There is significant evidence that wireless channels vary greatly over time and location [20, 21, 1, 15]. A common way to model this variance analytically is using a zero-mean Gaussian random variable with standard deviation σ, or X_σ. Although this model does not capture all real-world behavior, we use it here to simulate controllable levels of path-loss variance. We vary the σ value and compare the results in Figure 13. This figure shows the simulation results when we introduce non-zero X_σ value and use randomized antenna gain for each different node location. This figure implies that there are wide area where the CTX is unexpected or inconsistently available (effectively *gray regions* of CTXability).

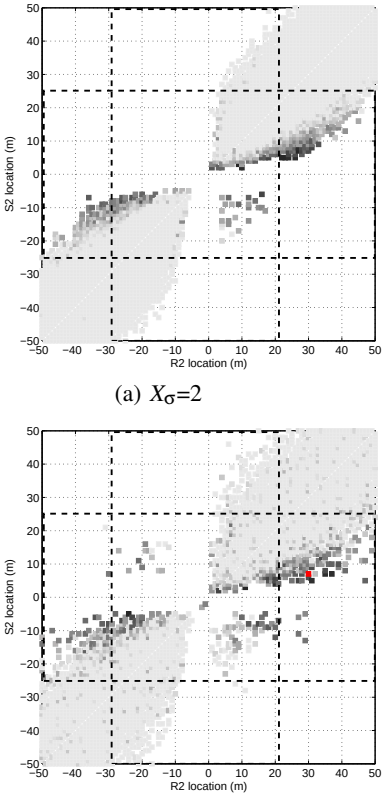

(a) X_σ=2

(b) X_σ=4

Figure 13. CTXable regions with different path loss variance X_σ **:** $S1, R1 = (-4, 0)$**,** $n = 4$**,** $SINR_\theta = 5$

In addition, we observe that cross-pair communication, where S2-R2 surround S1-R1, are more prevalent at higher path loss variance. We can observe the *SR* type communi-

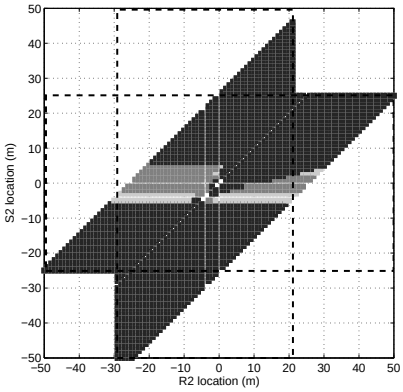

Figure 14. Capturable Regions. $S1, R1 = (-4, 0)$**,** $n = 4$**,** $SINR_\theta = 5$**,** $X_\sigma = 0$**,** $Tx\ power = 0\ dBm$

cation at $X_\sigma = 2$ (in Figure 13(a)), and both *SR* and *RS* type communication at $X_\sigma = 4$ (in Figure 13(b)). But, there is no cross-pair type communication for the same configuration (shown in Figure 10(b)) without path loss variance. We conclude that, in practice, CTXability will depend strongly on current environmental conditions.

5.6 Capturable Region

We mainly discussed about CTXable region in our simulation results. However, we observed large portion of power settings that allows only one successful communication under concurrent packet transmission (for example, we can see large S1 or S2 capture power settings in Figure 4). Understanding *capturable* situation is meaningful for both unicast and especially for broadcast communication.

Figure 14 presents CTXability obtained from the simulation with two concurrent packet senders S1 and S2, with corresponding (only for unicast communication) receivers R1 and R2. Both senders use a fixed transmission power of 0 *dBm*, which simulates the maximum power available for MicaZ motes. We indicate different types of capture regions in different colors. First, black color shows *unicast capture region* where at least one of unicast communications (S1-R1 or S2-R2) is successful; this combines both S1 and S2 *capturable regions*. Unicast capture regions cover 90% of the collision region. Gray color indicates the *broadcast capture region* where transmitted packet can be received by any neighbor node (i.e., either R1 or R2). This shows packet capture region under broadcast type of communication. This corresponds to 97% of the collision region (black region is a subset of gray region). Light gray color shows the collision region which does not allow any successful communication. There are only 3% of the collision region in which actual packet collision happens.

This simulation result implies that we can expect significant number of successful packet delivery under the traditional packet collision situation if MAC provides appropriate functionalities for concurrent packet communication (such as [18]).

6 Testbed Experiments

While the simulations in Section 5 are invaluable at systematically exploring the parameter space, multiple empirical studies suggest that analytic models do not capture the complexity in wireless propagation [1, 15, 20, 21].

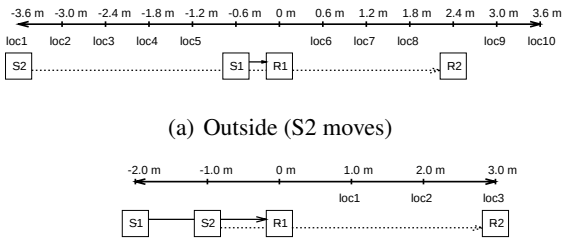

(a) Outside (S2 moves)

(b) Inside (R2 moves)

Figure 15. MicaZ experiment topology with two sender-receiver pairs. Experimented S1 locations: loc1–loc10 for scenario 1 and loc1–loc3 for scenario 2

We therefore next study key parameters in a testbed with real sensor nodes to verify the findings of our simulations. We use low-power MicaZ motes equipped with CC2420 radios [3] to measure the received signal and interference strength and to test the CTXability under concurrent packet transmission situation with different node topologies. The main objective of our experimental study is to demonstrate the feasibility of concurrent transmission in the real systems.

6.1 Methodology

Our testbed experiments follow the methodology of recent studies of concurrent transmission [16]. Like our simulation study, we use two sender-receiver pairs of nodes, S1-R1 and S2-R2. To coordinate the senders, our experiments add a fifth node, the *synchronizer*, that transmits a a packet to synchronize the concurrent packet senders. We disable carrier sensing and random backoff functionality from the MAC layer to allow concurrent packet transmission from multiple senders.

We consider two scenarios, *outside* and *inside*, as shown in Figure 15. In the outside scenario S2 is always outside the S1-R1 pair, and S2 moves. We vary the S2-R2 distance, considering ten different positions of S2, roughly every 60 cm. This scenario corresponds to cases *SR* and *RRA* in Figure 6(c). In the second experiment, *inside*, we place S2 between S1 and R1 so that the S2-R2 communication crosses S1-R1. We then move R2 to three positions, from 1 to 3 m beyond R1; this corresponds to the case *IR*.

The MicaZ supports 8 different transmission power levels from -25 to 0 dBm. For each position experiment, we first measure the signal and interference strength with 10 packets and then test the CTXability with 25 concurrent packet transmissions for every 64 different combinations of two senders' transmission power settings. We repeat the same experiment twice for each topology to verify that the results are consistent; the results were similar and we show only one experiment here due to space limitation.

6.2 Results from the Outside Scenario

Figure 16 shows the ability of nodes in our testbed to concurrently communicate (CTX) or capture the channel in our experiments at eight different locations of S2 (out of 10 due to space). Each figure shows 64 different CTXability

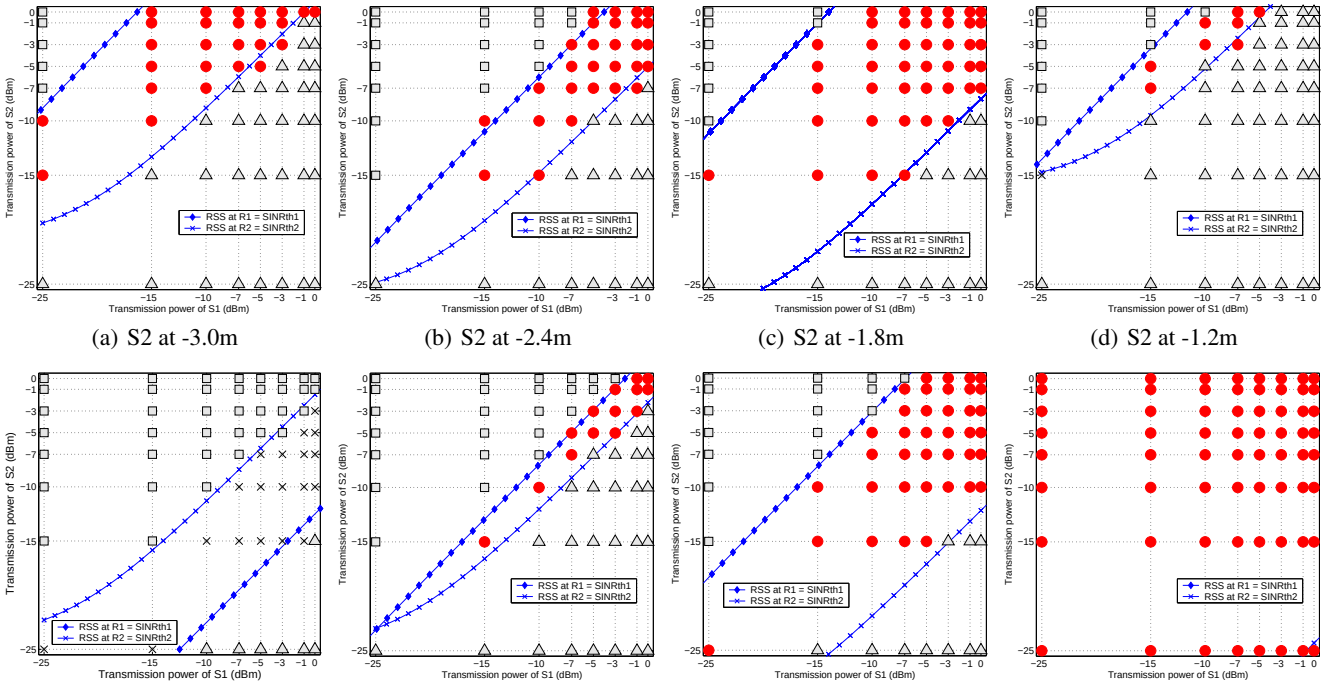

(a) S2 at -3.0m (b) S2 at -2.4m (c) S2 at -1.8m (d) S2 at -1.2m

(e) S2 at 0.6m (f) S2 at 1.2m (g) S2 at 1.8m (h) S2 at 3.0m

Figure 16. CTXability in the outside testbed experiment as S2 is moved (presented together with the expectation from simulation with our proposed formula) . Circles are *CTXable*, triangles and squares are *S1* or *S2 capturable*, and Xs indicate a collision. Simulation results at the same topology are presented together with two dotted lines.

tests with power of each of the two senders on each axis. These are all supported power combinations from two MicaZ senders. Results of each test are shown by different symbols: filled circles are CTXable, while empty triangles or squares indicate capture by S1 or S2, and Xs indicate collisions where neither receiver can capture data.

To compare our experiments with simulation, we predict the CTXable power settings through simulation and plot these as two lines (as in Figure 4). The simulations require parameters for the channel propagation model that we do not know, so we use actually measured path loss at each location using the data presented in Figure 17(b). We also used observed values for SINR threshold (*2 dB for MicaZ*) and ambient noise level for each node (-96.3 *dBm* for R1 and -96 *dBm* for R2). We can see that our simulation results provides very close match of experimentally observed CTXability. We will discuss the implication of this in Section 7.

Nine out of ten configurations supported concurrent communications at some power settings. Only R2 placement at 0.6 m (very close to R1) was unable to concurrently communicate. This experiment demonstrates the large opportunity for concurrent transmission if MAC support for packet capture and appropriate power selection was available, and RTS/CTS was revised. Nevertheless, current MAC protocols would prohibit many of these opportunities to transmit in their carrier sense checks or through an RTS/CTS handshake.

Figure 17(a) summarizes these experiments by comparing the number of power configurations that support CTXability, capture, or collision out of the 64 possible power combinations at each location. In some ways this the fraction of CTXable power combinations is not a useful metric, since an intelligent MAC would not select transmission power randomly, but instead could select whatever power level was best (so ideally, even a single CTXable configuration could be exploited). However, the percentage of CTXable configurations does characterize the level of flexibility in selecting transmission powers, the probability of a given outcome (CTX, capture, or collision) with a fixed power scheme, and perhaps the degree of tolerance to environmental noise and interference for each location.

We can also see from Figures 16 and 17(a) that even if two transmissions are not CTXable, almost always one or the other can be delivered with the capture effect. The SINR threshold of the MicaZ around 2 dB [16]. The low number of collisions in this experiment shows that it is rare for RSSs from both senders to fall within this 2 dB range. In our experiments, only 3% of power configurations resulted in collisions. This observation confirms our simulation results presented in Section 5.6. Older radios sometimes have larger SINR thresholds (the 2 to 6 dBm of the Mica2 [16]) and so may show larger collision regions.

To measure the effect of location on the signal and interference strength we plot the measured RSS and SINR values at fixed power level. (We expect the relationship to be inconsistent based on experience.) Figure 17(b) shows the measured received signal strength (RSS) for each pair S11, S22, I12, I21 at fixed transmission power level of -5 dBm, and

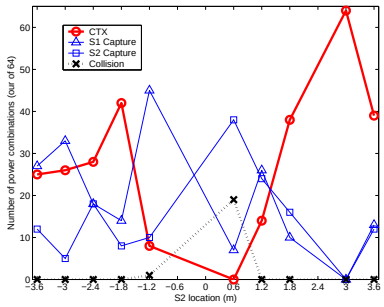

(a) CTXability

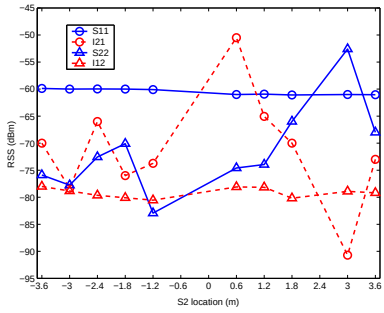

(b) RSS at $TxPwr = -5\ dBm$

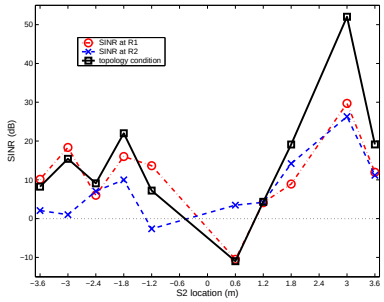

(c) SINR at $TxPwr = -5dBm$

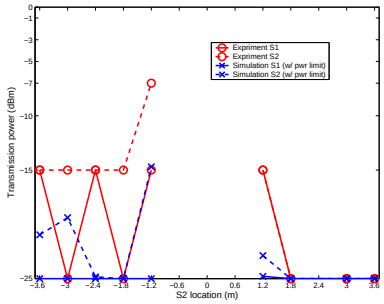

(d) Optimal transmission power

Figure 17. Experimental results at different S2 locations with variable transmission powers.

Figure 17(c) shows calculated SINR value at each receiver based on these measurements. First, we can see that measured RSS does not always correspond to link distance as we expect. This variation is due to environmental factors such as multi-path reflections.

We show the topology condition (the difference between the right hand side and the left hand side of the inequality in Equation 5) as the solid line. A positive value means topology condition is satisfied and the communication may be CTXable; as we can see this condition is only negative when S2 is 0.6 m, consistent with our findings in Figure 17(a). In Figure 17(c) we can observe one of the receiver does not satisfy 2 dB SINR threshold at the following three S2 locations: $-3\ m$, $-1.2\ m$, and $0.6\ m$. However, concurrent communications become possible with power control for every experiments other than S2 location at 0.6 m.

Figure 17(d) shows the optimal (i.e., minimum) transmission power selected for each sender S1 and S2 for concurrent communication based on our experiment results, together with optimal transmission power selected from our proposed formula (Equation 4), but with limited power range between -25 dBm and 0 dBm at 1 dBm intervals. We can see that experiments with S2 locations at -3 m, -1.8 m, and -1.2 m, which have much higher SINR at R1 (shown in Figure 17(c)), use higher optimal transmission power for S2 to redistribute leftover SINR (i.e., signal strength) value to make CTX possible. We can also see that the simulated optimal power matches our experiments. There is a difference in the plot, but this is coming from the limited power level support from our tested nodes (MicaZ), and nodes can choose the same power level as actual experiment based on simulation results.

6.3 Results from the Inside Scenario

In the second scenario in Figure 15(b), we place S2 inside the S1-R1 pair. Experiment results (presented in Figure 18) show that CTX is possible even with this configuration if nodes can control their transmission power. We observed that CTX is possible when R2 was at 2 m or 3 m in our experiments (presented in Figure 18(a)). However, we could not see any concurrent communication when R2 was at 1 m. This confirms what is predicted in simulation based on measured path loss; From Figure 18(b) we can see that topology condition fails only for location 1 m. This final case illustrates that locations, fails to satisfy topology condition, and limited transmission powers prevent CTXability in some cases.

These two testbed experiments confirm our key simulation results: first, that concurrent communication is highly probable in many previously restricted cases with traditional 802.11 like medium access control. Second, complete collisions and full corruption of both packets is rare and often at least one sender can capture a packet. Finally, controllable transmission power significantly improves CTXability.

7 Making CTXable Decisions in Practice

Section 4.3 described how we select optimal transmission powers to enable CTXablity when possible in simulation. Making this decision in practice is considerably more difficult for several reasons: the decision must be made at distributed nodes with little or no communication, node location is likely unavailable or inaccurate, and noise levels are constantly changing. Even if locations are known, distance is not an accurate estimator of signal and interference strength as we observe in our testbed experiments and others

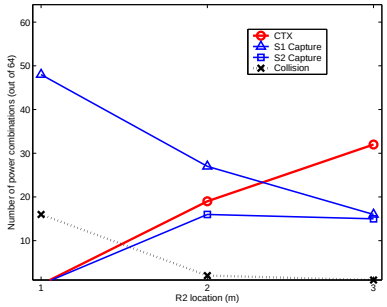

(a) CTXability

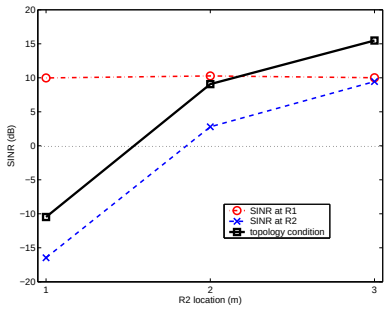

(b) SINR, TxPwr: 0 dBm

Figure 18. CTXability from the inside scenario

have observed in the past [1, 15, 20, 21].

However, if we can actually measure the path loss at a given location, we can avoid these real-world complexities and use this measurement directly our proposed formulae (Equation 4 and 5). This simplification is possible because these model parameters are used only to estimate path loss. Actual path loss information can be collected with a single RSS measurement at any transmission power level (*path loss* $=$ *Tx power* $-$ *RSS*), suggesting that a CTXable decision is feasible in real systems.

Our initial testbed experiments suggest a close match between simulation and testbed experiments (Figure 16). We are currently exploring a practical MAC that supports CTXability based on our findings in this paper.

8 Conclusions

In this paper we have presented the first effort to quantify the opportunity for concurrent communication in low-power wireless networks. We proposed a simple rule to determine when communication is CTXable and to select optimal transmission power given global knowledge or with measured path loss. Through simulation we systematically explored the parameter space, varying node position, mean and variance of path loss, signal-to-interference-plus-noise-ratio (SINR) threshold, range and granularity of transmission power control. We verified the key results of our simulations through testbed experiments with MicaZ motes, demonstrating that concurrent communication is often possible and capture by at least one receiver is almost always possible.

9 References

[1] D. Aguayo, J. Bicket, S. Biswas, G. Judd, and R. Morris. Link-level measurements from an 802.11b mesh network. In *ACM SIGCOMM*, aug 2004.

[2] V. Bharghavan, A. Demers, S. Shenker, and L. Zhang. MACAW: A media access protocol for wireless LAN's. pages 212–225, London, UK, Sept. 1994.

[3] Chipcon. Cc2420 2.4ghz ieee 802.15.4/ zigbee-ready rf transceiver.

[4] D. Couto, D. Aguayo, J. Bicket, and R. Morris. A high-throughput path metric for multi-hop wireless routing. In *IEEE Mobicom*, sep 2003.

[5] D. Ganesan, D. Estrin, A. Woo, D. Culler, B. Krishnamachari, and S. Wicker. Complex behavior at scale: An experimental study of low-power wireless sensor networks. Technical Report CS TR 02-0013, UCLA, 2002.

[6] K. Jamieson, B. Hull, A. Miu, and H. Balakrishnan. Understanding the real-world performance of carrier sense. In *SIGCOMM'05 Workshop*, aug 2005.

[7] A. Kochut, A. Vasan, A. Shankar, and A. Agrawala. Sniffing out the correct physical layer capture model in 802.11b. In *IEEE International Conference on Network Protocols (ICNP)*, oct 2004.

[8] D. Lal, A. Manjeshwar, F. Herrmann, E. Uysal-Biyikoglu, and A. Keshavarzian. Measurement and characterization of link quality metrics in energy constrained wireless sensor networks. In *IEEE Globecom*, dec 2003.

[9] S. Lin, J. Zhang, G. Zhou, L. Gu, T. He, and J. Stankovic. Atpc: Adaptive transmission power control for wireless sensor. In *Sensys*, nov 2006.

[10] T. Moscibroda. The worst-case capacity of wireless sensor networks. In *IPSN*, apr 2007.

[11] T. Moscibroda, R. Wattenhofer, and Y. Weber. Protocol design beyond graph-based models. In *HotNets-V*, nov 2006.

[12] V. Rajendran, K. Obraczka, and J. Garcia-Luna-Aceves. Energy-efficient, collision-free medium access control for wireless sensor networks. In *ACM Sensys*, nov 2003.

[13] T. Rappaport. *Wireless Communications: Principles and Practice*. Prentice Hall, 1996.

[14] C. Reis, R. Mahajan, M. Rodrig, D. Wetherall, and J. Zahorjan. Measurement-based models of delivery and interference in static wireless networks. In *ACM Sigcomm*, sep 2006.

[15] D. Son, B. Krishnamachari, and J. Heidemann. Experimental study of the effects of transmission power control and blacklisting in wireless sensor networks. In *IEEE SECON*, oct 2004.

[16] D. Son, B. Krishnamachari, and J. Heidemann. Experimental study of concurrent transmission in wireless sensor networks. In *ACM Sensys*, nov 2006.

[17] K. Srinivasan and P. Levis. Rssi is under appreciated. In *Emnets*, may 2006.

[18] K. Whitehouse, A. Woo, F. Jiang, J. Polastre, and D. Culler. Exploiting the capture effect for collision detection and recovery. In *IEEE Workshop on Embedded Networked Sensors (EmNetS-II)*, may 2005.

[19] J. L. Wong, L. Kuang, M. Potkonjak, and D. Estrin. Statistical model of lossy links in wireless sensor networks. In *IPSN*, apr 2005.

[20] A. Woo, T. Tong, and D. Culler. Taming the underlying challenges of reliable multihop routing in sensor networks. In *ACM Sensys*, nov 2003.

[21] J. Zhao and R. Govindan. Understanding packet delivery performance in dense wireless sensor networks. In *ACM Sensys*, nov 2003.

[22] G. Zhou, T. He, S. Krishnamurthy, and J. Stankovic. Impact of radio irregularity on wireless sensor networks. In *ACM MobiSys*, jun 2004.

[23] G. Zhou, T. He, J. Stankovic, and T. Abdelzaher. Rid: Radio interference detection in wireless sensor networks. In *IEEE Infocom*, mar 2005.

[24] M. Zuniga and B. Krishnamachari. Analyzing the transitional region in low power wireless links. In *IEEE SECON*, oct 2004.